

phenylenediamine with alloxan was examined. Again, an approximately equimolar mixture of two alloxazine products was obtained. Proton NMR spectra clearly demonstrated that one was VII, and the other was identical with VI. These results are summarized in Scheme II.

Taken together, the results discussed above demonstrate that the reaction of alloxan with substituted 2-amino-*N*-alkylanilines produces an alloxazine with reversed stereochemistry in addition to the expected flavin. No evidence for the alloxazine produced by N(10) dealkylation of the flavin has been observed. The most reasonable explanation for the observed products is that alloxan can condense with 2-amino-*N*-alkylanilines in either of two possible orientations. One produces the N(10)-alkylisalloxazine (flavin) directly, while the other yields an N(5)-alkylalloxazinium ion instead (Scheme I and II). Simple N(5)-dealkylation would yield an alloxazine with the observed stereochemistry. Although to our knowledge N(5)-alkylalloxazinium salts have not been prepared or detected directly, support for this hypothesis is afforded by a recent report on the chemistry of some closely related pterin derivatives.<sup>34</sup> Electrochemical oxidation of 5,6,6,7,7-pentamethyltetrahydropterin produces the N(5)-alkyldi-

hydropteridinium ion, which rapidly demethylates in aqueous solution to give the 6,6,7,7-tetramethyldihydropterin<sup>34</sup> in a reaction parallel to that which we propose.

Inasmuch as a variety of subtle steric and electronic effects are likely to dictate which nitrogen of an *N*-alkyl-*o*-phenylenediamine attacks the central carbonyl of alloxan most rapidly, it is difficult at this time to generalize about factors favoring formation of the flavin over the "reversed" alloxazine. Nonetheless, the availability of a competing route in the condensation reaction with concomitant formation of an alloxazine with solubility and chromatographic behavior quite different from that of the isalloxazine could well account for the highly variable yields encountered in classical flavin syntheses.<sup>4</sup> Conversely, a variety of substituted alloxazines could be available via this route by suitable choice of starting material.

**Acknowledgment.** This research was supported by grants to B.A.A. from the National Institutes of Health (GM32117 and GM28636).

**Supplementary Material Available:** Tables of observed and calculated structure amplitudes, anisotropic displacement parameters, and positional and isotropic displacement parameters for hydrogen atoms (29 pages). Ordering information given on any current masthead page.

(34) Eberlein, G.; Bruice, T. C.; Lazarus, R. A.; Henrie, R.; Benkovic, S. J. *J. Am. Chem. Soc.* 1984, 106, 7916-7924.

## Heteronuclear NMR Studies of Cobalamins. 4. $\alpha$ -Ribazole-3'-phosphate and the Nucleotide Loop of Base-on Cobalamins<sup>1</sup>

Kenneth L. Brown\* and Janette M. Hakimi

Contribution from the Department of Chemistry, The University of Texas at Arlington, Arlington, Texas 76019-0065. Received August 5, 1985

**Abstract:**  $\alpha$ -Ribazole-3'-phosphate (1- $\alpha$ -D-ribofuranosyl-5,6-dimethylbenzimidazole-3'-phosphate), the detached nucleotide of the nucleotide loop of cobalamins, has been prepared by sulfuric acid catalyzed hydrolysis of the phosphodiester of cyanocobalamin and characterized by <sup>1</sup>H, <sup>13</sup>C, and <sup>31</sup>P NMR of both the zwitterionic and dianionic forms. These NMR characteristics along with those of the cationic and neutral forms of  $\alpha$ -ribazole have been used to analyze trends in the <sup>13</sup>C NMR resonances of the nucleotide loops of a series of 10 base-on cobalamins in which the apparent strength of benzimidazole coordination varies by more than 6 orders of magnitude. Trends in the benzimidazole carbon resonances are found to be dominated by electronic and dipolar shielding effects and a method is developed for estimating the magnetic anisotropy ( $\Delta\chi$ ) of the cobalt atom dipole for cobalamins of known geometry. The ribose moiety chemical shifts are influenced by electronic and dipolar effects, and the ribose moiety appears to have a different conformation than that of the free nucleotide and nucleoside. Trends in the chemical shifts of the 2-hydroxypropylamine carbons and the trend previously reported for the phosphorus atom chemical shift are shown to be due primarily to regular changes in nucleotide loop conformation throughout the series of compounds. Two-bond and three-bond phosphorus-carbon coupling constants are consistent with this interpretation.

In recent publications,<sup>2-4</sup> we have investigated the <sup>31</sup>P NMR spectroscopy of cobalamins and showed that while all base-off cobalamins investigated have the same <sup>31</sup>P chemical shifts, the position of the <sup>31</sup>P resonance of base-on cobalamins varies directly with the apparent strength of coordination of the axial benzimidazole nucleotide. For this work, we have estimated the free energy of benzimidazole coordination  $\Delta G_{Co}$ , from eq 1, where the

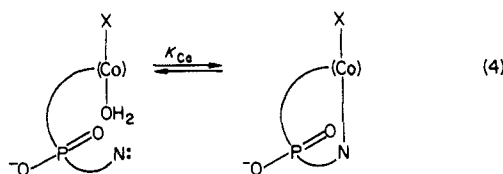
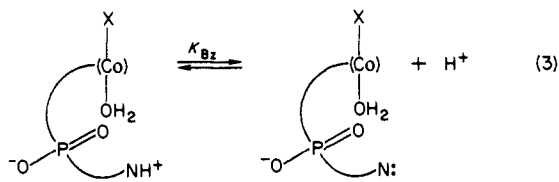
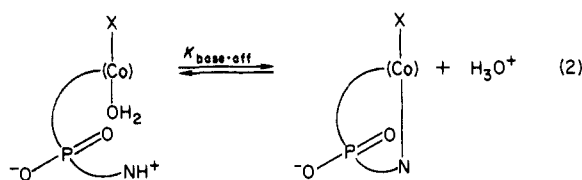
$$K_{\text{base-off}} = (1 + K_{Co})K_{Bz} \quad (1)$$

equilibrium constants are defined in eq 2-4, and  $pK_{Bz}$  is assumed to be equal to the  $pK_a$  of the detached benzimidazolium nucleoside

( $\alpha$ -ribazole,  $pK_a = 5.56$  at 25 °C, ionic strength 1.0 M).<sup>5</sup> Thus, the change in <sup>31</sup>P chemical shift upon displacement of the axial base by protonation ( $\Delta\delta_{31p} = \delta_{31p}^{\text{base-on}} - \delta_{31p}^{\text{base-off}}$ ) is directly proportional to  $-\Delta G_{Co}$ ,<sup>2</sup> for a series of 10 cobalamins in which  $K_{Co}$  (eq 4) varies over more than 6 orders of magnitude. In addition, for those cobalamins whose geometry is known from X-ray crystallography, the base-on <sup>31</sup>P chemical shift was shown to be directly related to the axial Co-N bond distance, the resonance moving downfield with decreasing Co-N bond distance (and increasing strength of coordination). These observations have been interpreted in terms of the work of Gorenstein and co-workers<sup>6-8</sup> who have shown that the <sup>31</sup>P chemical shift of phosphate

(1) For part 3, see ref 2.  
(2) Brown, K. L.; Hakimi, J. M.; Jacobson, D. W. *J. Am. Chem. Soc.* 1984, 106, 7894-7899.  
(3) Brown, K. L.; Hakimi, J. M. *Inorg. Chem.* 1984, 23, 1756-1764.  
(4) Brown, K. L.; Hakimi, J. M. *Inorg. Chim. Acta* 1982, 67, 229-231.

(5) Brown, K. L.; Hakimi, J. M.; Nuss, D. M.; Montejano, Y. D.; Jacobson, D. W. *Inorg. Chem.* 1984, 23, 1463-1471.  
(6) Gorenstein, D. G. *J. Am. Chem. Soc.* 1975, 97, 898-900.  
(7) Gorenstein, D. G.; Kar, D. *Biochem. Biophys. Res. Commun.* 1975, 65, 1073-1080.



esters and phosphodiester is largely (if not completely) controlled by phosphate conformation. We consequently suggested<sup>2</sup> that the increasing strength of coordination of the benzimidazole ligand, and the associated decrease in axial Co-N bond length, is accompanied by a regular change in nucleotide loop conformation including a small, but systematic, change in the O-P-O bond angle, leading to the observed changes in base-on <sup>31</sup>P chemical shift. Similar observations of trends in <sup>31</sup>P chemical shifts of base-on cobalamins have recently been made by Marzilli and co-workers<sup>9</sup> and interpreted similarly.

Such regular changes in nucleotide loop conformation throughout a series of base-on cobalamins should be accompanied by changes in <sup>13</sup>C chemical shifts of the carbon atoms of the nucleotide loop. The recent work of Hogenkamp and co-workers<sup>10,11</sup> leading to virtually complete assignment of the natural abundance <sup>13</sup>C NMR spectra of several cobalamins has now allowed us to determine if this is the case. In a general sense, any regular changes in the <sup>13</sup>C chemical shift of carbons in the nucleotide loop of a series of base-on cobalamins in which the benzimidazole ligand is increasingly tightly coordinated may be due to a combination of three effects: (i) changes in electronic effects due to increased forward donation of electron density from benzimidazole to cobalt with increasing strength of coordination, (ii) changes in dipolar shielding due to changes in the magnetic anisotropy of the induced dipole in the cobalt atom throughout the series of compounds, and (iii) changes in nucleotide loop conformation with increasing strength of coordination. Regarding the second factor, extensive NMR and structural studies of cobaloxime model complexes by Marzilli and co-workers<sup>12-15</sup> have shown that cobalt atom magnetic anisotropy has a large effect on chemical shifts of nearby atoms. These studies also suggest that changes in the upper axial ligand will have a much larger effect on the magnetic anisotropy of the cobalt atom than changes in the lower axial Co-N bond distance and that distortions of the equatorial ligand (due to bulky upper axial ligands) also significantly affect cobalt magnetic anisotropy.

In the work described in this paper, we have prepared  $\alpha$ -ribose-3'-phosphate (i.e., 1- $\alpha$ -D-ribofuranosyl-5,6-dimethylbenz-

imidazole-3'-phosphate), the detached axial nucleotide of the cobalamins, and studied its <sup>1</sup>H, <sup>31</sup>P, and <sup>13</sup>C NMR for direct comparison to the nucleotide loop of base-on cobalamins. In addition, we have attempted to quantitate the electronic and dipolar shielding effects for those cobalamins whose geometry is known from X-ray crystallography and consequently obtained additional evidence for conformational effects in the nucleotide loop.

## Experimental Section

Aquacobalamin (H<sub>2</sub>OCbl), cyanocobalamin (CNCbl), methylcobalamin (CH<sub>3</sub>Cbl), and 5'-deoxyadenosylcobalamin (AdoCbl) were from Sigma. All other organocobalamins were prepared (from aquacobalamin), purified, and characterized as previously described.<sup>5</sup>  $\alpha$ -Ribazole was also prepared as previously described.<sup>5</sup> All other reagents, solvents, etc., were obtained in the highest purity commercially available and used without further purification. Glass-distilled, deionized water was used throughout.

$\alpha$ -Ribazole-3'-phosphate was prepared by sulfuric acid catalyzed hydrolysis of cyanocobalamin, based on our previous observation of asymmetric, partial hydrolysis of the phosphodiester of CNCbl to produce two phosphomonoesters, i.e.,  $\alpha$ -ribose-3'-phosphate and cyanocobinamide phosphate,<sup>3</sup> subsequent hydrolysis of the phosphomonoesters to inorganic phosphate being much slower. It has previously been prepared by perchloric acid catalyzed hydrolysis of CNCbl.<sup>16-19</sup> Cyanocobalamin (2.0 g) was dissolved in 150 mL of 2.125 M aqueous sulfuric acid and incubated at 25 °C in the dark for 42 h. At this point, <sup>1</sup>H-coupled <sup>31</sup>P NMR showed the presence of two doublets (-51.75 Hz,  $J_{H-P} = 7.81$  Hz, 64% of total integral, and -88.86 Hz,  $J_{H-P} = 9.77$  Hz, 36% of total integral) and no evidence of a CNCbl triplet<sup>3,20,21</sup> or a singlet for inorganic phosphate. The solution was cooled in ice and the pH adjusted to 3.23 with NaOH. After several hours of stirring at room temperature in the dark, a large, gelatinous, red precipitate was filtered and washed with water. The combined filtrate and washings was extracted 6 times with 40 mL of liquified phenol, and the combined phenol extracts were carefully washed twice with 80-mL portions of water. The washed phenol extracts (ca. 240 mL) were diluted with 250 mL of acetone and 750 mL of ether and then back extracted with eight 70-mL portions of water. The back extract was washed 5 times with 10-mL portions of methylene chloride followed by five 10-mL portions of ether and concentrated to about 30 mL on a rotary flash evaporator. The pH (3.76) was adjusted to 3.20 with HCl. <sup>1</sup>H-coupled <sup>31</sup>P NMR showed two doublets, 26.36 Hz,  $J_{H-P} = 7.81$  Hz, 64% of total integral and 3.90 Hz,  $J_{H-P} = 9.76$ , 36% of total. This solution was then loaded onto a 2 × 20 cm column of Amberlite XAD-2 (Serva, 100-120 mesh) and eluted with water. After the first 385 mL of elute, material with an  $\alpha$ -ribose-like UV spectrum<sup>5</sup> began to emerge. A total of 4.5 L of elute was collected and the column was regenerated by washing (until colorless) with 50% aqueous acetonitrile, followed by water. The eluted  $\alpha$ -ribose-3'-phosphate was evaporated to dryness. The slightly pink solid was recrystallized from boiling water with the addition of hot acetone: yield, 352 mg as the zwitterion (65% based on total CNCbl). Anal. Calcd for C<sub>14</sub>H<sub>19</sub>N<sub>7</sub>O<sub>7</sub>P: C, 46.93%; H, 5.35%; N, 7.82%; P, 8.65%; O, 31.26. Found:<sup>22</sup> C, 46.77%; H, 5.44%; N, 7.61%; P, 8.96%; O, 31.22% (by difference) NMR. See Results and Discussion section.

UV-visible spectra were obtained on a Cary 219 recording spectrophotometer, and pH measurements were made on a Radiometer PHM 64 pH meter. NMR spectra were obtained on a Nicolet NT-200 wide-bore superconducting NMR spectrometer (4.7 T) operating at 80.988 (<sup>31</sup>P), 50.311 (<sup>13</sup>C), or 200.068 MHz (<sup>1</sup>H). All chemical shifts for <sup>1</sup>H and <sup>13</sup>C NMR were determined relative to internal DSS, while <sup>31</sup>P chemical shifts are relative to external 85% H<sub>3</sub>PO<sub>4</sub>. Positive chemical shifts are downfield from the reference. <sup>1</sup>H NMR spectra of  $\alpha$ -ribose and  $\alpha$ -ribose-3'-phosphate were obtained in D<sub>2</sub>O, while <sup>13</sup>C NMR spectra of cobalamins were obtained in D<sub>2</sub>O/H<sub>2</sub>O (20% D<sub>2</sub>O v/v) to provide a deuterium lock signal. <sup>13</sup>C NMR spectra were collected in 16K data sets over a 10 000-Hz sweep width using 7.5- $\mu$ s 30° pulses, an 819-ms acquisition time, a 2.0-s cycle delay, and bilevel (1.0 and 2.5 W) broad-band noise-modulated proton decoupling. Anywhere from 50 000 to 80 000 transients were collected on 3.0-mL samples containing 40-80

(8) Gorenstein, D. G. *J. Am. Chem. Soc.* **1977**, *99*, 2254-2258.

(9) Rossi, M.; Glusker, J. P.; Randaccio, L.; Summers, M. F.; Toscano, P. J.; Marzilli, L. G. *J. Am. Chem. Soc.* **1985**, *107*, 1729-1738.

(10) Anton, D. L.; Hogenkamp, H. P. C.; Walker, T. E.; Matwiyoff, N. A. *Biochemistry* **1982**, *21*, 2372-2378.

(11) Bratt, G. T.; Hogenkamp, H. P. C. *Biochemistry* **1984**, *23*, 5653-5659.

(12) Trogler, W. C.; Stewart, R. C.; Epps, L. A.; Marzilli, L. G. *Inorg. Chem.* **1974**, *13*, 1564-1570.

(13) Stewart, R. C.; Marzilli, L. G. *Inorganic Chem.* **1977**, *16*, 424-427.

(14) Trogler, W. C.; Marzilli, L. G. *J. Am. Chem. Soc.* **1974**, *96*, 7589-7591.

(15) Trogler, W. C.; Marzilli, L. G. *Inorg. Chem.* **1975**, *14*, 2942-2948.

(16) Friedrich, W.; Bernhauer, K. Z. *Naturforsch.*, **B 1954**, *9b*, 685-694.

(17) Friedrich, W.; Bernhauer, K. Z. *Naturforsch.*, **B 1956**, *11b*, 68-73.

(18) Lezius, A. G.; Barker, H. A. *Biochemistry* **1965**, *4*, 510-518.

(19) Friedman, H. C. *J. Biol. Chem.* **1968**, *243*, 2065-2075.

(20) Satterlee, J. D. *Biochem. Biophys. Res. Commun.* **1979**, *89*, 272-278.

(21) Satterlee, J. D. *Inorg. Chim. Acta* **1980**, *46*, 157-166.

(22) Galbraith Laboratories, Knoxville, TN.

Table I.  $^1\text{H}$  and  $^{13}\text{C}$  NMR Data for  $\alpha$ -Ribazole<sup>a</sup>

atom	neutral (pD 7.5)			cation (pD 3.0)		
	$\delta_{\text{H}}$	$J$ , Hz	$\delta_{^{13}\text{C}}$	$\delta_{\text{H}}$	$J$ , Hz	$\delta_{^{13}\text{C}}$
B2	n.o. <sup>b</sup>		n.o. <sup>b</sup>	9.206		140.791
B4	7.504		121.299	7.503		116.517
B5			135.232			140.038
B6			134.017			139.835
B7	7.379		113.731	7.445		114.938
B8			136.124			131.099
B9			142.929			131.317
B10	2.358		22.207	2.383		22.354
B11	2.342		21.910	2.362		22.173
R1	6.334	$J_{1-2} = 4.00$	88.895	6.475	$J_{1-2} = 4.60$	90.081
R2	4.555	$J_{2-3} = 4.40$	74.178	4.788	$J_{2-3} = 4.84$	74.130
R3	4.435	$J_{3-4} = 7.20$	73.073	4.465	$J_{3-4} = 5.39$	73.372
R4	4.368	$J_{4-5A} = 4.30$ $J_{4-5B} = 2.60$	85.859	4.556	$J_{4-5A} = 4.60$ $J_{4-5B} = 3.00$	88.035
R5A	3.777	$J_{5A-5B} = 12.55$	63.677	3.842	$J_{5A-5B} = 12.49$	63.851
R5B	3.924			3.983		

<sup>a</sup> In  $\text{D}_2\text{O}$   $25 \pm 1^\circ\text{C}$ . All chemical shifts relative to internal DSS. <sup>b</sup> Not observed, see text.

Table II.  $^1\text{H}$  and  $^{13}\text{C}$  NMR Data for  $\alpha$ -Ribazole-3'-phosphate<sup>a</sup>

atom	dianion (pD 8.6) <sup>b</sup>			zwitterion (pD 3.0) <sup>c</sup>		
	$\delta_{\text{H}}$	$J$ , Hz	$\delta_{^{13}\text{C}}$	$\delta_{\text{H}}$	$J$ , Hz	$\delta_{^{13}\text{C}}$
B2	8.411		145.647	9.132		140.732
B4	7.458		121.255	7.412		116.464
B5			135.104			139.958
B6			134.226			139.785
B7	7.352		113.699	7.179		115.129
B8			136.058			131.245
B9			142.870			131.375
B10	2.314		22.202	2.294		22.355
B11	2.293		21.918	2.213		22.145
R1	6.381	$J_{1-2} = 4.20$	88.506	6.411	$J_{1-2} = 5.40$	89.779
R2	4.712 <sup>d</sup>		74.093 <sup>e</sup>	4.956	$J_{2-3} = 5.00$	74.247 <sup>f</sup>
R3	4.712 <sup>d</sup>	$J_{3-4} = 5.40$	75.746 <sup>g</sup>	4.842	$J_{3-4} = 4.00$	76.989 <sup>h</sup>
R4	4.517	$J_{4-5A} = 4.40$ $J_{4-5B} = 3.30$	85.933 <sup>i</sup>	4.595	$J_{4-5A} = 4.10$ $J_{4-5B} = 2.70$	88.668 <sup>j</sup>
R5A	3.881	$J_{5A-5B} = 12.65$	63.881	3.854	$J_{5A-5B} = 12.70$	63.859
R5B	3.951			3.953		

<sup>a</sup> In  $\text{D}_2\text{O}$ ,  $25 \pm 1^\circ\text{C}$ . All chemical shifts relative to internal DSS. <sup>b</sup>  $\delta_{^{31}\text{P}} = 373.1$  Hz from external 85%  $\text{H}_3\text{PO}_4$ ,  $J_{\text{R3H-P}} = 6.00$  Hz. <sup>c</sup>  $\delta_{^{31}\text{P}} = 29.0$  Hz from external 85%  $\text{H}_3\text{PO}_4$ ,  $J_{\text{R3H-P}} = 7.81$  Hz. <sup>d</sup> Unresolved multiplet at 200 MHz. <sup>e</sup>  $J_{\text{ocop}} = 2.36$  Hz. <sup>f</sup>  $J_{\text{ocop}} = 4.83$  Hz. <sup>g</sup>  $J_{\text{ocop}} = 4.28$  Hz. <sup>h</sup>  $J_{\text{ocop}} = 5.03$  Hz. <sup>i</sup>  $J_{\text{ocop}} = 5.79$  Hz. <sup>j</sup>  $J_{\text{ocop}} = 2.82$  Hz.

mg of cobalamin. For chemical shift determinations signal-to-noise ratios were enhanced by use of exponential multiplication (line broadening 1.0 Hz), but phosphorus-carbon coupling constants were determined from transients transformed without exponential multiplication.

In order to obtain a sufficiently concentrated sample of free-base  $\alpha$ -ribazole for  $^1\text{H}$  NMR and minimize interference from the solvent signal,  $\alpha$ -ribazole was preexchanged with  $\text{D}_2\text{O}$  by dissolving 10 mg in 3.0 mL of 99.8%  $\text{D}_2\text{O}$ . This solution was evaporated to dryness, and the residue plus 1.7 mg of DSS was redissolved in 99.8%  $\text{D}_2\text{O}$ . This solution was evaporated to dryness and the residue was dissolved in 3.0 mL of 100%  $\text{D}_2\text{O}$  (Aldrich Gold Label). This solution was concentrated to about 0.75 mL, and the resulting supersaturated solution was used for  $^1\text{H}$  NMR spectroscopy. Following  $^1\text{H}$  NMR measurements, the solution was diluted to 3.0 mL with 99.8%  $\text{D}_2\text{O}$  and used for  $^{13}\text{C}$  NMR. Unfortunately under these conditions, the B2 proton (see below) exchanged with solvent so that neither the B2 proton or carbon resonance could be observed. For the cationic form of  $\alpha$ -ribazole ( $\text{pK} = 5.56^5$ ), 84 mg of  $\alpha$ -ribazole and 3.5 mg of DSS were stirred in 2.95 mL of 99.8%  $\text{D}_2\text{O}$  and the mixture titrated to pD 3.0 with 20%  $\text{DCl}/\text{D}_2\text{O}$  (99 atom % D, Aldrich) to effect the solution. The solution was used for both  $^1\text{H}$  and  $^{13}\text{C}$  NMR. For the  $\alpha$ -ribazole-3'-phosphate dianion, 50 mg of the zwitterion and 5 mg of DSS were stirred with 3.0 mL of 99.8%  $\text{D}_2\text{O}$  and titrated to pD 8.6 with 40%  $\text{NaOD}/\text{D}_2\text{O}$  (Aldrich) to dissolve the  $\alpha$ -ribazole-3'-phosphate. This solution was used for  $^{13}\text{C}$  NMR. In order to minimize the solvent peak for  $^1\text{H}$  NMR, this sample was evaporated to dryness, redissolved in 99.8%  $\text{D}_2\text{O}$ , and evaporated to dryness again. This procedure was repeated once more and the final residue dried overnight over  $\text{P}_2\text{O}_5$  in vacuo. The dry residue was dissolved in 1.0 mL of 100%  $\text{D}_2\text{O}$  for  $^1\text{H}$  NMR. For the  $\alpha$ -ribazole-3'-phosphate zwitterion which is only poorly soluble in water, a supersaturated solution at pD 3.0 was prepared as follows. A dried, exchanged sample of the dianion was prepared as above and then dissolved in 1.0 mL of 100%  $\text{D}_2\text{O}$ . This solution was evaporated to dryness and dried over  $\text{P}_2\text{O}_5$  in vacuo over-

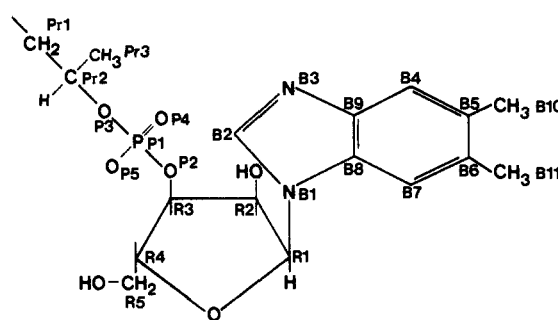


Figure 1. Structure and numbering scheme for the nucleotide loop of cobalamins.

night. The residue was dissolved in 1.0 mL of 100%  $\text{D}_2\text{O}$  and carefully titrated to pD 3.0 with 20%  $\text{DCl}$  in 100%  $\text{D}_2\text{O}$ . The resulting supersaturated solution was stable for at least 8 h. A similar solution was prepared in a 3.0-mL volume (with 99.8%  $\text{D}_2\text{O}$ ) for  $^{13}\text{C}$  NMR.

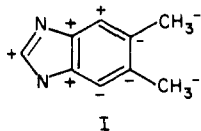
## Results and Discussion

Figure 1 shows the structure and standard numbering scheme for the nucleotide loop of cobalamins. For convenience, the same numbering scheme will be used to discuss the NMR properties of the detached benzimidazole nucleoside and nucleotide.  $^{13}\text{C}$  and  $^1\text{H}$  NMR chemical shifts and coupling constants for the neutral (pD 7.5) and cationic (pD 3.0) forms of  $\alpha$ -ribazole are listed in Table I, and similar data (including  $^{31}\text{P}$  chemical shifts and H-P and P-C coupling constants) are listed in Table II for the  $\alpha$ -ribazole-3'-phosphate dianion (pD 8.6) and zwitterion (pD 3.0).<sup>23</sup>

$^1\text{H}$  NMR assignments were made by chemical shift, relative integrals, multiplicity, and selective decoupling experiments, while  $^{13}\text{C}$  assignments were made by chemical shifts, intensity, multiplicity in off-resonance decoupling experiments, and selective continuous-wave proton decoupling. Unfortunately, the R2 and R3 proton resonances of the dianion of  $\alpha$ -ribose-3'-phosphate were unresolvable at 200 MHz, appearing as a multiplet centered at 4.712 ppm. In addition, the procedure used to replace exchangeable hydrogens with deuterons in order to minimize the solvent signal in the  $^1\text{H}$  and  $^{13}\text{C}$  NMR samples of neutral  $\alpha$ -ribose caused complete exchange of the B2 proton so that neither the resonance of this proton nor the resonance of the B2 carbon could be observed. Surprisingly, a similar treatment of the  $\alpha$ -ribose-3'-phosphate dianion did not cause significant exchange of the B2 proton.

Comparison of the  $^{13}\text{C}$  resonances of neutral  $\alpha$ -ribose with those of the  $\alpha$ -ribose-3'-phosphate dianion and of the resonances of cationic  $\alpha$ -ribose with those of the  $\alpha$ -ribose-3'-phosphate zwitterion readily shows the effects of substitution of a phosphate dianion at R3 of B3-deprotonated  $\alpha$ -ribose and substitution of a phosphate monoanion at R3 of B3-protonated  $\alpha$ -ribose. In both cases, the effects of phosphate substitution on the  $^{13}\text{C}$  resonances of the benzimidazole moiety are extremely small, the largest effect being a 0.191 ppm downfield shift of the B7 resonance upon substitution of a phosphate monoanion on B3-protonated  $\alpha$ -ribose. All other  $^{13}\text{C}$  chemical shift changes in the benzimidazole moiety upon phosphate substitution at R3 are less than 0.15 ppm regardless of the ionization state at B3, and most are less than 0.1 ppm. For the B3-deprotonated species, phosphate dianion substitution at R3 causes upfield shifts of all the benzimidazole resonances except B6 and B11, while for B3-protonated species phosphate monoanion substitution at R3 causes upfield shifts of the B2, B4, B5, B6, and B11 resonances, while B7, B8, B9, and B10 move downfield. A larger effect of phosphate ion substitution is, of course, observed for the ribose carbon resonances. Even so, except for R3 (the point of substitution), the effects are quite small. Thus, for B3-deprotonated species, while phosphate dianion substitution causes a 2.67 ppm downfield shift of R3, R1 and R2 move upfield by 0.39 and 0.09 ppm, respectively, and R4 and R5 move downfield by 0.07 and 0.20 ppm, respectively. Phosphate monoanion substitution on the B3-protonated species has larger effects on R2, R3, and R4 but smaller effects on R1 and R5. Thus, R1 moves upfield 0.30 ppm, while R2, R3, R4, and R5 all move downfield by 0.12, 3.62, 0.63, and 0.01 ppm, respectively.

Comparison of the  $^{13}\text{C}$  chemical shifts of neutral and cationic  $\alpha$ -ribose and dianionic and zwitterionic  $\alpha$ -ribose-3'-phosphate allows quantitation of the effect of B3 protonation on the  $^{13}\text{C}$  spectrum, of obvious relevance to anticipated electronic effects on the  $^{13}\text{C}$  NMR of the nucleotide loop of a series of cobalamins characterized by increasing strength of coordination of B3 to cobalt. For both the nucleoside and nucleotide, B3 protonation causes substantial upfield shifting of the  $^{13}\text{C}$  resonances of B2, B4, B8, and B9, while B5, B6, B7, B10, and B11 are all shifted downfield. This pattern of chemical shift changes upon B3 protonation is summarized in I, in which the sign of the difference in chemical shift between the B3-deprotonated and B3-protonated species is given for each benzimidazole carbon. The effects of



(23) The implicit assumption is that the isoelectric point of  $\alpha$ -ribose-3'-phosphate is near 3.0. This is based on the assumption that the first macroscopic  $pK$  (expected to be essentially identical with the microscopic  $pK$  for phosphate ionization from the monocation) will be around 1.0<sup>24</sup> and the second macroscopic  $pK$  will be above 5.0. The latter assumption is based on the fact that the second macroscopic  $pK$  is expected to be dominated by the microscopic  $pK$  for B3 ionization from the zwitterion, and the analogous  $pK$  for  $\alpha$ -ribose is 5.56.<sup>5</sup>

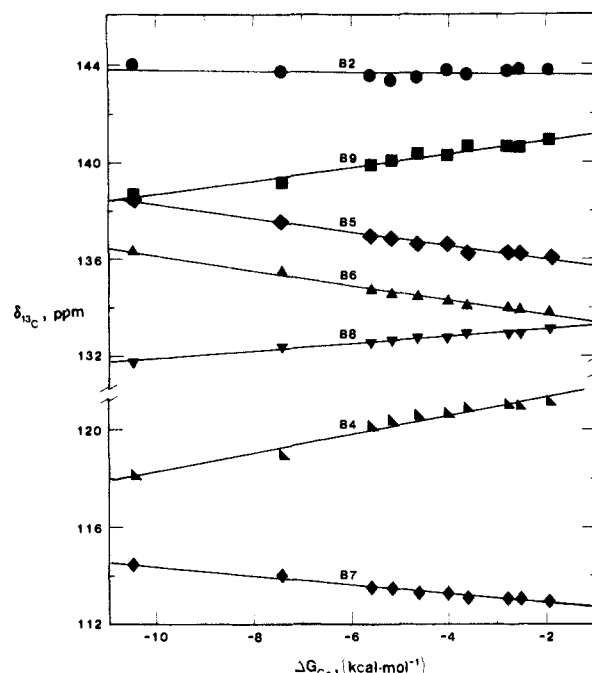


Figure 2. Plots of the  $^{13}\text{C}$  chemical shift,  $\delta_{13\text{C}}$ , of the benzimidazole carbons of the nucleotide loop of the base-on cobalamins vs.  $\Delta G_{\text{Co}}$  (eq 1 and 4), the apparent free energy of coordination of benzimidazole to cobalt. The solid lines are least-squares fits, the slopes of which are listed in Table III.

B3 protonation on the ribose carbon chemical shifts are much smaller with the exception of R1 and R4 which are shifted downfield by more than 1.0 and more than 2.0 ppm, respectively. While the effect on R1 may reasonably be attributed to electronic influences, R4, six bonds removed from B3, is too remote from the site of protonation to be experiencing only an electronic effect (i.e., the chemical shift differences at R2 and R3 of  $\alpha$ -ribose upon B3 protonation are much smaller despite closer proximity to the site of protonation). The relatively large change in R4 chemical shift upon B3 protonation may well indicate a conformational change (either in the ribose moiety itself or in the  $\alpha$ -N-glycosidic bond) upon B3 protonation.

With these NMR characteristics of the benzimidazole nucleotide and nucleoside in mind, we may now turn our attention to the  $^{13}\text{C}$  NMR of the nucleotide loop of base-on cobalamins. Table III lists the  $^{13}\text{C}$  chemical shifts of the 17 carbons in the nucleotide loop for 10 base-on cobalamins along with the measured<sup>2,5</sup> values of  $pK_{\text{base-off}}$  (eq 2) and calculated values of  $K_{\text{Co}}$  and  $\Delta G_{\text{Co}}$  (eq 1) for each cobalamin. Also given are least-squares slopes for the linear correlations of the chemical shift with  $\Delta G_{\text{Co}}$ . Without exception, the chemical shifts reported for CNCbl, H<sub>2</sub>OcbI, CH<sub>3</sub>Cbl, and AdoCbl are virtually identical with those previously reported by Hogenkamp and co-workers,<sup>10,11</sup> after correction is made for the difference in chemical shift between internal DSS (this work) and external TMS.<sup>10,11</sup> Note that the apparent affinity of the benzimidazole nucleotide for the cobalt atom (i.e.,  $K_{\text{Co}}$ ) in this series varies by more than 6 orders of magnitude. Trends in the chemical shifts of the various carbon atoms throughout the series are readily recognized and are depicted graphically via plots of chemical shift vs.  $\Delta G_{\text{Co}}$  in Figure 2 (for the benzimidazole carbons) and Figure 3 (for the ribose and 2-hydroxypropylamine carbons). Excepting the benzimidazole methyl groups (B10 and B11), which behave anomalously, all the benzimidazole carbons show large trends in chemical shift throughout the series with the exception of B2 for which the trend is negligible (Figure 2). In addition, all the ribose and 2-hydroxypropylamine carbons (Figure 3) except R2 and R5 also show significant, although smaller, trends throughout the series. For these carbons, the difference in chemical shift between the extremes of the series (i.e., *n*-propylcobalamin and aquocobalamin) is at least 0.28 ppm and for all except Pr3 exceeds 0.46 ppm. For

Table III.  $^{13}\text{C}$  NMR Chemical Shifts of the Nucleotide Loop of Base-on Cobalamins<sup>a</sup>

atom	$\text{CH}_3(\text{CH}_2)_2\text{Cbl}$	AdoCbl	$\text{NC}(\text{CH}_2)_3\text{Cbl}$	$\text{CH}_3\text{Cbl}$	$\text{CF}_3\text{CH}_2\text{Cbl}$	$\text{CF}_2\text{HCbl}$
B2	144.229	144.202	144.266	144.401	144.235	144.507
B4	121.175	120.975	120.985	120.826	120.616	120.598
B5	136.073	136.268	136.296	136.276	136.641	136.634
B6	133.851	133.965	133.991	134.060	134.286	134.391
B7	112.994	113.046	113.061	113.039	113.245	113.251
B8	133.123	132.935	132.973	132.966	132.746	132.798
B9	140.930	140.596	140.675	140.663	140.225	140.368
B10	22.160	23.523	22.901	22.584	23.670	22.866
B11	21.917	23.142	22.179	22.329	22.230	22.242
R1	88.855	88.921	88.954	88.952	89.179	89.167
R2	75.448	75.457	75.438	75.457	75.445	75.458
R3	75.793	75.658	75.614	75.610	75.574	75.608
R4	84.083	84.029	84.025	84.025	84.105	84.145
R5	63.023	62.961	62.938	62.996	62.883	62.955
Pr1	47.415	47.387	47.352	47.497	47.531	47.576
Pr2	71.811	71.655	71.652	71.613	71.526	71.501
Pr3	21.324	21.377	21.389	21.392	21.401	21.443
$pK_{\text{base-off}}^c$	4.10	3.67	3.50	2.89	2.60	2.15
$K_{\text{Co}}^d$	$2.80 \times 10^1$	$7.66 \times 10^1$	$1.15 \times 10^2$	$4.67 \times 10^2$	$9.23 \times 10^2$	$2.60 \times 10^3$
$\Delta G_{\text{Co}}^d$ kcal mol <sup>-1</sup>	-1.97	-2.57	-2.81	-3.64	-4.04	-4.66

atom	$\text{NCCH}_2\text{Cbl}$	$\text{CF}_3\text{Cbl}$	$\text{CNCbl}$	$\text{H}_2\text{OCbl}$	slope, <sup>b</sup> ppm/kcal
B2	144.667	144.454	144.306	144.028	$0.0150 \pm 0.0245$
B4	120.305	120.104	118.941	118.117	$0.380 \pm 0.025$
B5	136.824	136.950	137.582	138.454	$-0.282 \pm 0.014$
B6	134.568	134.716	135.502	136.342	$-0.306 \pm 0.016$
B7	113.448	113.475	113.968	114.449	$-0.182 \pm 0.012$
B8	132.648	132.526	132.396	131.760	$0.151 \pm 0.010$
B9	140.034	139.883	139.161	138.647	$0.277 \pm 0.020$
B10	22.421	22.301	22.410	23.741	
B11	22.288	21.960	21.894	22.448	
R1	89.296	89.400	89.519	89.979	$-0.133 \pm 0.007$
R2	75.433	75.408	75.446	75.448	$0.00881 \pm 0.00202$
R3	75.590	75.561	75.550	75.329	$0.0293 \pm 0.0062$
R4	84.229	84.307	84.513	84.854	$-0.101 \pm 0.009$
R5	62.895	62.933	62.951	62.906	$0.00833 \pm 0.0053$
Pr1	47.673	47.828	47.919	48.052	$-0.0897 \pm 0.0094$
Pr2	71.445	71.378	71.381	71.226	$0.0624 \pm 0.0081$
Pr3	21.490	21.432	21.596	21.608	$-0.0345 \pm 0.0043$
$pK_{\text{base-off}}^c$	1.81	1.44	0.10	-2.13	
$K_{\text{Co}}^d$	$6.40 \times 10^3$	$1.32 \times 10^4$	$2.88 \times 10^5$	$4.90 \times 10^7$	
$\Delta G_{\text{Co}}^d$	-5.19	-5.62	-7.44	-10.48	

<sup>a</sup> In  $\text{H}_2\text{O}/\text{D}_2\text{O}$  (5:1  $\nu/\nu$ ),  $25 \pm 1^\circ\text{C}$ . All chemical shifts relative to internal DSS. <sup>b</sup> Slope of the linear correlation of  $\delta_{^{13}\text{C}}$  with  $\Delta G_{\text{Co}}$ . <sup>c</sup> Equation 2. <sup>d</sup> Calculated from  $pK_{\text{base-off}}$  and eq 1, using  $pK_{\text{Bz}} = 5.56$ .<sup>2,5</sup>

the benzimidazole carbons, with the exception of B2, all the trends in carbon chemical shift with increasing axial base affinity are in the same direction as the change in chemical shift of the same carbon atom in  $\alpha$ -ribazole or  $\alpha$ -ribazole-3'-phosphate upon B3 protonation, suggesting, as anticipated, a significant electronic effect on the benzimidazole carbons due to increased electron donation from B3 to cobalt throughout the series. However, there is also significant evidence of other effects. For instance, with the exception of B6, all the benzimidazole chemical shifts of the base-on cobalamins fall within the range of values delineated by the B3-deprotonated and B3-protonated nucleoside and nucleotide (Tables I and II). However, for some of the benzimidazole carbons, such as B8, the chemical shifts of all of the base-on cobalamins fall closer to that of the B3-protonated form of the detached nucleotide and nucleoside, while for others, like B9, the chemical shifts of the base-on cobalamins fall closer to that of the B3-deprotonated forms of the detached nucleotide and nucleoside. For B6, the observed values for several of the base-on cobalamins fall outside the range delineated by the B6 chemical shift of B3-protonated and -deprotonated  $\alpha$ -ribazole and  $\alpha$ -ribazole-3'-phosphate. These observations suggest that something other than the electronic effect has a significant influence on the chemical shifts of carbon atoms in the nucleotide loop of base-on cobalamins.

In general, trends in the chemical shifts of the carbon atoms of the nucleotide loop of the base-on cobalamins with increasing  $K_{\text{Co}}$  can be attributed to combination of three effects: (i) electronic effects due to increased forward donation of electron density from B3 to cobalt with increasing strength of coordination throughout

the series; (ii) trends in the remote heavy atom effect (due to the magnetic anisotropy of the induced dipole in the cobalt atom) due to changes in geometry as well as changes in the magnitude of the magnetic anisotropy of the induced dipole throughout the series of compounds; and (iii) changes in nucleotide loop conformation with increasing strength of coordination throughout the series. As the relative magnitude of these three effects varies considerably for the different components of the nucleotide loop, the trends in chemical shift of each component will be discussed separately.

**The Benzimidazole Moiety.** It seems unlikely that the benzimidazole moiety would undergo significant changes in conformation throughout the series of cobalamins, a supposition which is supported by examination of the X-ray crystal structures of AdoCbl,<sup>25</sup>  $\text{CH}_3\text{Cbl}$ ,<sup>9</sup> and  $\text{CNCbl}$ .<sup>26,27</sup> Consequently, only electronic and dipolar shielding effects need to be considered. Importantly, Trogler and Marzilli<sup>15</sup> have concluded that magnetic anisotropy of the equatorial ligand of cobaloximes is not an important contributor to chemical shift trends in the axial ligands of these  $\text{B}_{12}$  model complexes. It therefore seems reasonable to attribute all the dipolar shielding effects in the base-on cobalamins to magnetic anisotropy of the cobalt atom. The effects of cobalt

(24) McElroy, W. D.; Glass, B. "Phosphorus Metabolism"; Johns Hopkins University Press: Baltimore, 1951; Vol. 1.

(25) Lenhart, P. G. *Proc. R. Soc. London, Ser. A* 1968, 303, 45-84.

(26) Brink-Shoemaker, C.; Cruickshank, D. W. J.; Hodgkin, D. C.; Kamper, M. J.; Pilling, D. *Proc. R. Soc. London, Ser. A* 1964, 278, 1-26.

(27) Hodgkin, D. C.; Lindsey, J.; Sparks, R. A.; Trueblood, K. N.; White, J. G. *Proc. R. Soc. London, Ser. A* 1962, 266, 494-517.

Table IV. Calculated Chemical Shifts and Anisotropic Shielding Factors for Certain Base-on Cobalamins

atom	AdoCbl		CH <sub>3</sub> Cbl		"wet" CNCbl		"dry" CNCbl	
	$\delta_{13C}^{calcd a}$	$\Delta\sigma^b$	$\delta_{13C}^{calcd a}$	$\Delta\sigma^b$	$\delta_{13C}^{calcd a}$	$\Delta\sigma^b$	$\delta_{13C}^{calcd a}$	$\Delta\sigma^b$
B2	142.706	2.489	142.690	2.331	142.855	0.630	142.761	0.738
B4	119.990	0.825	119.955	0.691	118.983	0.165	118.996	0.165
B5	135.245	0.289	135.429	0.271	137.088	0.075	137.077	0.073
B6	134.446	0.307	134.663	0.292	136.665	0.082	136.655	0.076
B7	113.387	0.443	113.459	0.422	114.201	0.127	114.203	0.121
B8	134.589	1.027	134.505	0.940	133.652	0.289	133.646	0.308
B9	139.695	2.120	139.326	2.082	137.130	0.685	137.191	0.655
B10		0.016		0.045		0.013		0.008
B11		0.149		0.133		0.039		0.034
R1		0.415		0.392		0.107		0.115
R2		0.294		0.279		0.080		0.082
R3		0.144		0.136		0.037		0.039
R4		0.131		0.115		0.026		0.035
R5		0.049		0.049		0.010		0.014
Pr1		-0.018		-0.021		-0.006		-0.006
Pr2		+0.0002		-0.0002		-0.001		-0.0005
Pr3		-0.002		-0.003		-0.0007		-0.0005
P1		0.046		0.043		0.012		0.012
1 - $\alpha$		0.091		0.127		0.440		0.437
$\Delta\chi$ , $\times 10^{29}$ cm <sup>3</sup> /molecule		-14.3		-13.1		-3.35		-3.45
$\Delta G_{Co}$ , <sup>c</sup> kcal mol <sup>-1</sup>		-2.57		-3.64		-7.44		-7.44

<sup>a</sup>Chemical shifts, in ppm, calculated from eq 6 as described in the text. <sup>b</sup>Anisotropic shielding calculated from eq 5 and the determined values of  $\Delta\chi$ . <sup>c</sup>Calculated from eq 1 and the measured values of  $pK_{base-off}$  (eq 2<sup>25</sup>), assuming  $pK_{Bz}$  to be 5.56.<sup>5</sup>

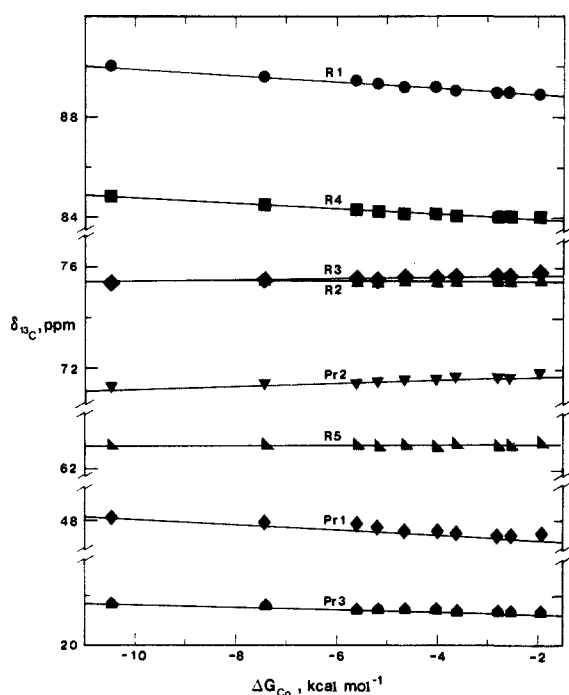


Figure 3. Plots of the <sup>13</sup>C chemical shifts,  $\delta_{13C}$ , of the ribose and 2-hydroxypropylamine carbons of the nucleotide loop of the base-on cobalamins vs.  $\Delta G_{Co}$  (eq 1 and 4), the apparent free energy of coordination of benzimidazole to cobalt. The solid lines are least-squares fits, the slopes of which are listed in Table III.

dipole magnetic anisotropy may be quantitated by assuming an axially symmetric point dipole by use of McConnell's equation (eq 5<sup>28</sup>), where  $\Delta\sigma$  is the observable shielding,  $\Delta\chi$  is the magnetic

$$\Delta\sigma = \Delta\chi (1 - 3 \cos^2 \theta) / 3R^3 \quad (5)$$

anisotropy of the induced dipole (i.e., the difference between the magnetic susceptibility parallel ( $\chi_{||}$ ) and perpendicular ( $\chi_{\perp}$ ) to the dipole symmetry axis),  $R$  is the distance between the cobalt atom and the observed nucleus, and  $\theta$  is the angle between the dipole symmetry axis and the vector  $R$ . If the symmetry axis of the induced dipole is assumed to lie along the pseudo-C<sub>4</sub> axis,<sup>12</sup>

then for complexes of known geometry (i.e., AdoCbl, CH<sub>3</sub>Cbl, and CNCbl), the dipolar shielding may be estimated from eq 5 provided that a value of  $\Delta\chi$  is available. However, as detailed above, the benzimidazole moiety <sup>13</sup>C resonances are clearly subject to substantial changes in electronic effect throughout the series. To the extent that coordination of benzimidazole B3 to cobalt resembles "partial protonation" of  $\alpha$ -ribazole or  $\alpha$ -ribazole-3'-phosphate at B3 (the assumption being that coordination is dominated by forward  $\sigma$ -electron donation from nitrogen to cobalt, i.e., cobalt-to-nitrogen back donation is negligible) then both the electronic and dipolar shielding effects can be quantitated via eq 6, where  $\delta^{obsd}$  is the observed chemical shift of a particular ben-

$$\delta^{obsd} = (\delta^{rib} - \delta^{ribH^+})\alpha + \delta^{ribH^+} - \Delta\chi(1 - 3 \cos^2 \theta) / 3R^3 \quad (6)$$

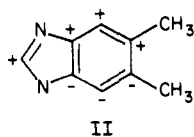
zimidazole carbon in the nucleotide loop of a base-on cobalamin,  $\delta^{rib}$  and  $\delta^{ribH^+}$  are the chemical shifts of the same carbon atom in the appropriate ionic species of B3-deprotonated and B3-protonated  $\alpha$ -ribazole-3'-phosphate, respectively, and  $1 - \alpha$  represents the degree of apparent "partial protonation" of benzimidazole due to coordination to cobalt in that particular cobalamin. Although appropriate values of  $\delta^{ribH^+}$  are available as the chemical shifts of the benzimidazolium moiety of the  $\alpha$ -ribazole-3'-phosphate zwitterion, values of  $\delta^{rib}$  should be those of the  $\alpha$ -ribazole-3'-phosphate monoanion in which B3 is deprotonated and the phosphate moiety is monoanionic. Unfortunately, the NMR spectrum of this monoanion cannot be obtained as it is at all times in rapid tautomeric equilibrium with the monoanionic species in which B3 is protonated and the phosphate moiety is dianionic. However, as pointed out above, the presence of either monoanionic or dianionic phosphate at R3 causes very little change in the position of the benzimidazole <sup>13</sup>C resonances of both B3-protonated and -deprotonated  $\alpha$ -ribazole. Consequently, we cannot make too large an error if we use the  $\alpha$ -ribazole-3'-phosphate dianion chemical shifts for  $\delta^{rib}$  values in eq 6.

For cobalamins of known geometry for which  $R$  and  $\theta$  can be calculated from atomic coordinates, eq 6 contains two unknowns (i.e.,  $\alpha$  and  $\Delta\chi$ ) so that any pair of <sup>13</sup>C resonances may be used to calculate values of  $\alpha$  and  $\Delta\chi$ . Since there are 7 observable resonances in the benzimidazole nucleus, 21 pairwise calculations may be made and the average value of  $\alpha$  and  $\Delta\chi$  used as the best estimates. Such calculations have been carried out for the three cobalamins whose structures have been determined by X-ray crystallography (i.e., AdoCbl,<sup>25</sup> CH<sub>3</sub>Cbl,<sup>9</sup> and both the "wet"<sup>26</sup> and "dry"<sup>27</sup> CNCbl structures) assuming that the cobalt dipole symmetry axis lies along the normal to the least-squares plane of the equatorial nitrogens (and through the cobalt atom),<sup>29</sup> and

(28) McConnell, H. M. *J. Chem. Phys.* 1957, 27, 226-229.

the results are shown in Table IV. In addition to the calculated values of  $1 - \alpha$  and  $\Delta\chi$ , Table IV also shows the calculated chemical shifts for the benzimidazole nucleus carbons for these four cobalamins as well as the calculated values of  $\Delta\sigma$ , the dipolar shielding, for all the NMR observable nuclei of the nucleotide loop. It must, however, be stressed that the calculations can only be considered to be approximate in that the assumption that the electronic effect on the benzimidazole  $^{13}\text{C}$  chemical shifts can be treated as the fractional equivalent of protonation at B3 is untested by independent means and can only be considered as an approximation. Nonetheless, the results are quite encouraging in several respects. First, the calculated values of  $\Delta\chi$  compare well to a value of  $-7.3 \times 10^{-29} \text{ cm}^3/\text{molecule}$  previously obtained by Stewart and Marzilli for a cobaloxime model system.<sup>13</sup> Second, the extent of apparent "partial protonation" of the benzimidazole ligand at B3 increases monotonically with increasing strength of coordination (i.e., decreasing  $\Delta G_{\text{Co}}$ ). Third, as expected, the magnetic susceptibility parallel to the dipole symmetry axis ( $\chi_{\parallel}$ ) decreases relative to the perpendicular component (i.e.,  $\Delta\chi$  becomes less negative) as the trans axial ligand becomes an increasingly strong field ligand. It is, however, interesting to note that the value of  $\Delta\chi$  for AdoCbl is very similar to that for  $\text{CH}_3\text{Cbl}$ . As Trogler and Marzilli<sup>15</sup> have concluded that bulky axial ligands in cobaloxime models cause significant changes in cobalt magnetic anisotropy (via distortion of the equatorial ligand), this suggests that the 5'-deoxyadenosyl ligand is not particularly bulky compared to the methyl ligand. A similar conclusion (at least in the solid state) has recently been reached via comparison of the overall corrin conformation of AdoCbl and  $\text{CH}_3\text{Cbl}$  from the X-ray crystal structures.<sup>9</sup>

In general, the fit between the calculated and observed chemical shifts for the benzimidazole moiety carbons is reasonably good (Table IV). With a few exceptions, the largest errors in calculated chemical shift are for the carbon atoms closest to the metal atom as anticipated by McConnell due to the breakdown of the point dipole approximation at close range.<sup>28</sup> Interestingly, the signed errors (calculated as  $\delta^{\text{obsd}} - \delta^{\text{calcd}}$ , II), with the exception of B4 for both forms of CNCbl which have a negligibly small error at B4, show a pattern very similar to the change in chemical shift upon protonation of the nucleoside or nucleotide at B3 (i.e., I), the only differences between being inversion of the sign at B5 and B8. This suggests that a systematic error has been made in



accounting for the electronic effect and may imply that the assumption of insignificant Co-to-N back bonding is incorrect.

At any rate, the estimates of  $\Delta\chi$  in Table IV allow us to appreciate the magnitude of the dipolar shielding effect on the chemical shifts of the benzimidazole carbons. For cobalamins with weak field upper axial ligands (such as Ado and  $\text{CH}_3$ ), the effect can be very large, ranging from nearly 2.5 ppm for B2 to about 0.3 ppm for B6, the most distant benzimidazole carbon. The effect is very much smaller for cobalamins with strong field upper axial ligands (represented by CNCbl) where the largest effect (B2) is less than 1.0 ppm.

**The Ribose Moiety.** Unfortunately, the inability to obtain a  $^{13}\text{C}$  NMR spectrum of the appropriate monoanion of  $\alpha$ -ribose-3'-phosphate precludes a detailed analysis of the trends in chemical shift of the ribose moiety. However, several points regarding the ribose moiety can be made from the data on hand. All the ribose carbons except R2, which shows virtually no trend,

and R5, for which the small trend is probably not statistically significant, do show substantial trends of at least 0.45 ppm throughout the series. The trend in R1 chemical shifts, the largest of the five carbons, is probably largely electronic in nature. This can be appreciated from the change in the R1 chemical shift upon protonation of  $\alpha$ -ribose at B3 (Table I), which amounts to about 1.2 ppm. From Table IV, the difference in extent of "partial protonation" between CNCbl and AdoCbl is about 0.34 so that about 34% of the 1.2 ppm (ca. 0.4 ppm) difference in the R1 chemical shift might be expected between AdoCbl and CNCbl from the electronic effect alone. However, correcting for the expected difference in dipolar shielding in R1 for the two complexes (Table IV) increases the anticipated difference to 0.6 ppm. This is almost exactly the observed difference in R1 chemical shift between AdoCbl and CNCbl. Unfortunately, the confounding influence of the R3 phosphate substituent on the other ribose carbon chemical shifts precludes such an analysis for these carbons.

The dipolar shielding effect (Table IV) can be seen to be very much smaller for the ribose carbons than for the benzimidazole carbons, as expected. While for AdoCbl and  $\text{CH}_3\text{Cbl}$  all the values of  $\Delta\sigma$  exceed 0.1 ppm except that for R5, for CNCbl the  $\Delta\sigma$  values are all less than 0.1 ppm except that of R1. However, careful comparison of the ribose chemical shifts of the base-on cobalamins (Table III) with those of the various ionic species of  $\alpha$ -ribose and  $\alpha$ -ribose-3'-phosphate (Tables I and II) show that some important influence other than electronic and dipolar shielding effects is involved. While the R1, R3, and R5 chemical shifts of the base-on cobalamins seem reasonable compared to the detached nucleoside and nucleotide (taking both electronic and dipolar shielding effects into account), all the R2 shifts are about 1.5 ppm downfield from their expected positions and all the R4 shifts are at least 1.5 ppm upfield of their expected positions. These differences cannot be due to dipolar shielding effects as seen in Table IV. This suggests that there is a gross difference in the ribose ring conformation between the base-on cobalamins and the detached nucleoside and nucleotide. In the solid state, both the "dry" and "wet" CNCbl structures are known to have C(2)-exo ribose conformations, while the ribose moiety of AdoCbl is C-(3)-endo,<sup>30</sup> although no apparent discontinuities are seen in the ribose chemical shifts throughout the series of base-on cobalamins (Figure 3), suggesting that this change in ribose conformation (if it is relevant to solution conformations) must be gradual. Consequently, it is not possible to conclude that regular changes in ribose conformation accompany changes in axial ligand affinity throughout the series of compounds, although trends in phosphorus-carbon coupling constants (see below) suggest that this is probably the case.

**The Phosphorus Atom.** The phosphorus atom of the nucleotide loop is seven bonds removed from B3, the site of coordination, making it unlikely that the electronic effect of increased strength of coordination throughout the series could significantly affect the  $^{31}\text{P}$  chemical shifts. For perspective, R5, which is also seven bonds removed from B3, undergoes a change in chemical shift of 0.174 ppm upon protonation of  $\alpha$ -ribose at B3 (Table I). Since the difference in extent of apparent "partial protonation" of B3 for AdoCbl and CNCbl is about 0.34 (Table IV), the anticipated change in R5 chemical shift due to the electronic effect alone is about 0.06 ppm. The  $^{31}\text{P}$  chemical shifts of AdoCbl and CNCbl,<sup>2,3</sup> however, differ by 45.4 Hz or 0.56 ppm (at 80.988 MHz). As the range of  $^{31}\text{P}$  chemical shifts across the whole series of compounds is 0.735 ppm,<sup>2</sup> it seems unlikely that electronic effects can account for more than a small portion of this trend.

As the phosphorus atom also lies at least 9.0 Å from the cobalt atom and at an angle of approximately 40° with respect to the assumed symmetry axis of the cobalt dipole, the calculated dipolar shielding terms for the phosphorus atom are also very small (Table IV). Specifically, the difference in magnetic anisotropy of the cobalt dipole between AdoCbl and CNCbl can only account for 0.034 ppm (2.75 Hz) of the difference in  $^{31}\text{P}$  chemical shift (0.56 ppm or 45.4 Hz). We conclude, in agreement with our earlier

(29) Similar calculations have been carried out assuming the symmetry axis of the cobalt dipole lies along the axial Co-N bond and assuming this axis lies along the axial Co-C bond. The choice of the orientation of the dipole symmetry axis has very little effect on the results. For example, for  $\text{CH}_3\text{Cbl}$ ,  $\Delta\chi$  was  $-12.7 \times 10^{-29} \text{ cm}^3/\text{molecule}$  and  $1 - \alpha$  was 0.129 for the axial Co-N symmetry axis, and  $\Delta\chi$  was  $-13.7 \times 10^{-29} \text{ cm}^3/\text{molecule}$  and  $1 - \alpha$  was 0.123 for the Co-C symmetry axis.

(30) Sundaralingam, M. *Biopolymers* 1969, 7, 821-860.

Table V. Phosphorus–Carbon Coupling Constants for the Nucleotide Loop of Base-on Cobalamins<sup>a</sup>

RCbl	$\Delta G_{Co}$ , kcal mol <sup>-1</sup>	R4 ( $J_{CCOP}$ )	R3 ( $J_{COP}$ )	R2 ( $J_{CCOP}$ )	Pr1 ( $J_{CCOP}$ )	Pr2 ( $J_{COP}$ )	Pr3 ( $J_{CCOP}$ )
CH <sub>3</sub> (CH <sub>2</sub> ) <sub>3</sub> Cbl	-1.97	9.4	5.6	7.3	n.o. <sup>b</sup>	4.4	4.7
AdoCbl	-2.57	8.4	5.5	6.5	3.0	4.1	4.7
NC(CH <sub>2</sub> ) <sub>3</sub> Cbl	-2.81	7.8	5.5	6.8	3.4	3.7	4.2
CH <sub>3</sub> Cbl	-3.64	8.0	5.2	6.3	3.5	4.3	4.4
CF <sub>3</sub> CH <sub>2</sub> Cbl	-4.04	4.9	7.0	6.7	3.7	3.9	5.1
CF <sub>2</sub> HCbl	-4.66	8.4	4.7	6.2	4.1	n.o. <sup>b</sup>	3.9
NCCH <sub>2</sub> Cbl	-5.19	7.5	4.7	6.1	4.3	4.3	4.0
CF <sub>3</sub> Cbl	-5.62	7.6	4.2	6.3	4.6	3.9	3.2
CNCbl	-7.44	7.5	4.2	6.4	5.1	3.3	2.8
H <sub>2</sub> OCbl	-10.48	7.0	2.9	6.0	6.2	3.0	2.1

<sup>a</sup>Values in hertz. Conditions as for Table III. <sup>b</sup>Not observed.

speculation,<sup>2,3</sup> that the trend in <sup>31</sup>P chemical shift throughout the series of cobalamins is largely due to regular changes in phosphodiester conformation with increasing strength of coordination (and decreasing Co–B3 bond distance) throughout the series.

**The 2-Hydroxypropylamine Moiety.** The 2-hydroxypropylamine carbons are even more remote from B3, Pr2 being nine bonds removed and Pr1 and Pr3 being ten bonds removed, making the possibility of any significant electronic effect extremely small. Moreover, these carbons lie approximately 9.7, 9.2, and 11.3 Å, respectively, from the cobalt atom and make angles with the cobalt dipole symmetry axis very close to the magic angle. Consequently, the dipolar shielding of these carbons (Table IV) is negligibly small. Nevertheless, these carbons show substantial trends in chemical shift (Figure 3, Table III) throughout the series of compounds, Pr2 showing a trend of nearly 0.6 ppm, while Pr1 changes by 0.64 ppm and Pr3 by 0.28 ppm across the series. It is necessary to conclude that these chemical shift trends are largely, if not exclusively, due to changes in nucleotide loop conformation across the series of compounds.

**Phosphorus–Carbon Coupling Constants.** Both two-bond<sup>31–33</sup> and three-bond<sup>31,34,35</sup> phosphorus–carbon coupling constants are known to be stereospecific and show Karplus-like dihedral angle dependence. It must, however, be pointed out that in the current case, phosphorus–carbon coupling constants are difficult to determine with great accuracy. This is due in part to the crowding of the <sup>13</sup>C spectrum at 50.311 MHz (particularly the near overlap of R2 and R3) and the necessary limitations on digital resolution imposed by the necessity of collecting data on a broad sweep width

in a data set of reasonable size. Nonetheless, observed two-bond ( $J_{cop}$ ) and three-bond ( $J_{ccop}$ ) coupling constants for the nucleotide loop of the base-on cobalamins are shown in Table V to two significant figures, although the absolute accuracy is probably more like  $\pm 0.5$  Hz. For the most part (although with some notable exceptions, particularly for  $J_{cop}$  for Pr2), these results are in good agreement with the coupling constants previously reported by Bratt and Hogenkemp<sup>11</sup> for several of these cobalamins. Inspection of Table V shows that apparently significant trends in phosphorus–carbon coupling constants do occur for at least some of the carbon atoms, although there are some anomalous values in each series. However, it has been pointed out that it is not, in general, possible to relate such trends directly to specific changes in dihedral angles since separate correlations of  $J_{p(x),c}$  are likely to exist for each structural class.<sup>31</sup>

In conclusion, we have shown that careful analysis of the significant trends in <sup>13</sup>C chemical shifts of the carbon atoms of the nucleotide loop of a series of base-on cobalamins characterized by a regular increase in affinity of the benzimidazole B3 nitrogen for the cobalt atom of over 6 orders of magnitude in general allows at least a qualitative separation of inductive, conformational, and dipolar shielding effects. In this manner, significant evidence of regular changes in nucleotide loop conformation throughout the series of compounds has been obtained.

**Acknowledgment.** This research was supported by the Robert A. Welch Foundation, Houston, TX Grant Y-749. We are grateful to Prof. Dennis S. Marynick (Chemistry Department, UTA) for assistance with geometry calculations and for numerous helpful discussions.

**Registry No.** CNCbl, 68-19-9; CH<sub>3</sub>(CH<sub>2</sub>)<sub>2</sub>Cbl, 13985-72-3; AdoCbl, 13870-90-1; NC(CH<sub>2</sub>)<sub>3</sub>Cbl, 89414-81-3; CH<sub>3</sub>Cbl, 13422-55-4; CF<sub>3</sub>CH<sub>2</sub>Cbl, 21180-98-3; CF<sub>2</sub>HCbl, 69496-07-7; NCCH<sub>2</sub>Cbl, 92670-11-6; CF<sub>3</sub>Cbl, 31532-05-5; H<sub>2</sub>OCbl, 13422-52-1;  $\alpha$ -ribazole 3'-phosphate, 1098-68-6;  $\alpha$ -ribazole, 132-13-8.

(31) Gorenstein, D. G. *Prog. NMR Spectrosc.* **1983**, *16*, 1–98.

(32) Mavel, G. *Ann. Rep. NMR Spectrosc.* **1973**, *5b*, 1–94.

(33) McFarlane, W.; Nash, J. A. *J. Chem. Soc. Chem. Commun.* **1969**, 127–128.

(34) Quin, L. D.; Gallagher, M. J.; Cunkle, G. T.; Chesnut, D. B. *J. Am. Chem. Soc.* **1980**, *102*, 3136–3143.

(35) Duncan, M.; Gallagher, M. *J. Org. Magn. Reson.* **1981**, *15*, 37–42.